MARS THERMAL INERTIA FROM THEMIS DATA. N. E. Putzig, M. T. Mellon, B. M. Jakosky, S. M. Pelkey, S. Martínez-Alonso, B. M. Hynek, and N. W. Murphy, Laboratory for Atmospheric and Space Physics, University of Colorado, Boulder, CO 80309.

Introduction: As part of a Jet Propulsion Laboratory (JPL) Critical Data Products (CDP) initiative [1], we have developed a new technique for deriving thermal inertia from the Mars Odyssey (MO) Thermal Emission Imaging System (THEMIS) data. Our algorithm employs a modified version of the standard software developed for deriving thermal inertia from Mars Global Surveyor (MGS) Thermal Emission Spectrometer (TES) data [2]. This approach avoids complicating the comparison of THEMIS and TES results with thermal model differences. While THEMIS data provide greater than an order of magnitude improvement in spatial resolution over TES data, large uncertainties in calculated thermal inertias are introduced by a 5-fold increase in NEΔT (noise equivalent temperature uncertainty) for THEMIS [3] and by the lack of coincident-resolution albedo, elevation, and dust opacity. The higher resolution also complicates THEMIS data by increasing the role of surface slopes. Our analysis shows non-uniform differences between THEMIS and TES results, highlighting the need to calibrate THEMIS-derived thermal inertias from individual images against the more reliable TES-derived values.

Background: Thermal inertia is the key surface property controlling diurnal temperature variations and is dependent on the particle size, degree of induration, rock abundance, and exposure of bedrock within the top few centimeters of the subsurface. It is defined as the combination of thermal conductivity k, density ρ, and heat capacity C of the surface layer such that:

$$I \equiv \sqrt{k \rho C}\ .$$

Thermal inertia is a measure of the subsurface's ability to store heat during the day and to re-radiate it during the night. In general, unconsolidated fines will have low values of thermal inertia, indurated dust and sand-sized particles will have intermediate values, and rocks and exposed bedrock will have high values. For observations made from orbit, the thermal inertia of any given location on the surface is controlled by a variable mixture of such materials on the scale of the instrument resolution (~3 km for TES and ~100 m for THEMIS).

Methodology: We use a radiative-conductive thermal model of the martian atmosphere and near-surface regolith to calculate a lookup table of surface and brightness temperatures for a wide range of values for seven parameters: time of day, season, latitude, surface pressure, albedo, dust opacity, and thermal inertia. For each observed surface and brightness temperature, we obtain values for the first six of these parameters which coincide with the observation, using spacecraft ephemeris to determine time of day, season, and latitude, and using maps of other instrument data to determine surface pressure, albedo, and dust opacity. We then interpolate through the lookup table to obtain the best-fitting thermal inertia.

A lookup table and interpolation algorithm developed previously for TES data analysis [2] have been in use throughout the MGS primary and extended missions to derive thermal inertias from TES temperature data. The algorithm uses the MGS ephemeris and maps of elevation from MOLA (1º per pixel; for scaling Viking data [4] to surface pressure) and albedo from the TES visible bolometer (1/4º per pixel). When the algorithm was developed, time-varying atmospheric opacities were not expected to be available, so a constant IR dust opacity of 0.1 is assumed. Total uncertainties for the derived thermal inertia were estimated to be 6% for the bolometer and 17% for the spectrometer [2].

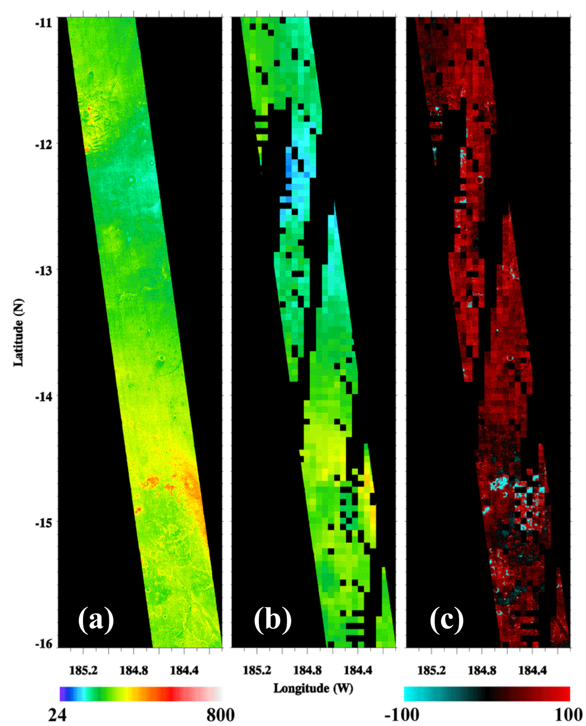

Figure 1: Thermal inertia (in J m^{-2} K^{-1} s$^{-1/2}$) over the MER Spirit landing site in Gusev Crater from (a) processing of THEMIS image I01511006 band-9 brightness temperatures and (b) a portion of the unfilled global map derived from TES nighttime bolometric temperatures [5]. (c) Thermal inertia difference (a − b) map clipped at ±100 (full range is −91 to 436).

A global map [5] of thermal inertias binned at 3 km was created using TES bolometer nighttime data from orbits 1583-11254 (L_s 103º-360º and 0º-152º) and employing filters to eliminate observations from periods of high water-ice-cloud and atmospheric-dust opacity.

We have modified the interpolation algorithm to use THEMIS band-9 brightness temperature images and emphemeris data from the MO spacecraft. In an effort to provide the best possible resolution for the JPL CDP initiative, we incorporated 1/20º per pixel MOLA elevation and TES albedo maps. Additionally, we extracted opacities from the TES database [6] to construct dust histories for each study region, using these to determine an opacity value near the time of observation for each THEMIS image. Despite these enhancements, the ancillary data resolution remains insufficient to characterize variations in their respective parameters on the 100-m scale of the THEMIS observations. Combined with the instrument uncertainty mentioned above, this prevents a reduction of uncertainty in THEMIS thermal inertia results to TES levels.

Results: For the JPL CDP project [1], we processed 156 THEMIS band-9 brightness temperature images through our new algorithm to obtain thermal inertias over the MER (Gusev and Meridiani) and Beagle 2 (Isidis) landing sites. Figure 1 compares the results for one THEMIS image with those derived from TES [5] over the same area, which crosses the MER Spirit landing site in Gusev Crater. Dramatic improvement in spatial resolution is evident in the THEMIS product while retaining the gross features seen in the TES map. The difference map shows that for this image, the THEMIS-derived values are generally higher than those from TES by about 30-100 J m^{-2} K^{-1} s$^{-1/2}$ (thermal inertia units, hereinafter abbreviated as 'tiu'). Figure 2 shows a 2-D histogram comparing the thermal inertia values from Figures 1a and 1b. The high range of scatter (−91 to +436 tiu) is indicative of local extremes of thermal inertia which become detectable at THEMIS resolution and is typical of other images. The trend of the elongated histogram peak nearly parallels the 1:1 line, indicating a good correspondence between the spatial variations in thermal inertia. However, the peak is offset by about 30-60 tiu above the 1:1 line. Other images we have analyzed show similar and larger offsets (up to about 120 tiu), in some cases below the 1:1 line (i.e., THEMIS lower than TES thermal inertias). This suggests that the error in the THEMIS results may be on the order of 25% for the images examined. These image-to-image variations are evident in mosaics of THEMIS thermal inertias which we created for each landing site for the JPL CDP initiative. Geological analysis of these mosaics together with TES thermal inertias and other data for Gusev [7], Meridiani [8], and Isidis [9] will be presented elsewhere at this conference.

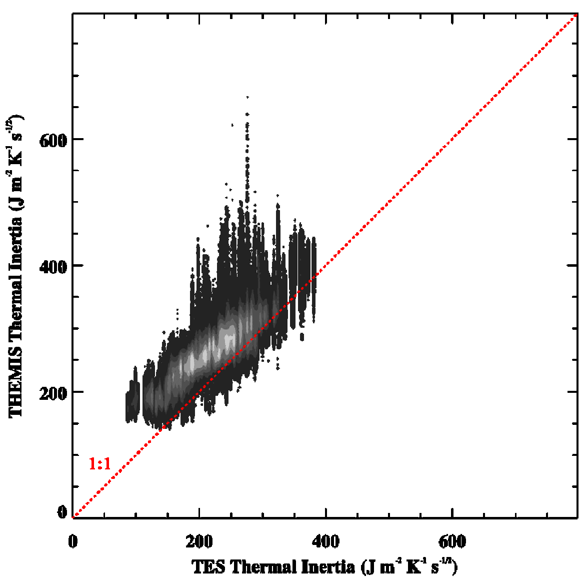

Figure 2: 2-D histogram of THEMIS image I1511006 and TES thermal inertias shown in Figure 1. The gray scale ranges from 1 to 1422 locations (100-m pixels) per histogram bin (3 J m^{-2} K^{-1} s$^{-1/2}$). Points on the 1:1 line represents perfect agreement.

The ancillary data resolution improvements made to optimize THEMIS results complicate comparison to TES results. We expect that albedo and elevation differences increase the scatter seen in Figure 2 but do not contribute substantially to the offset. Small registration errors between the datasets would have similar effects. Because the amplitude of the diurnal temperature cycle varies inversely with thermal inertia and dust opacity [2], systematic uncertainties in dust opacity could cause such an offset. While we account for dust opacities measured near the time of THEMIS observations, the average of opacities associated with TES observations may vary regionally from the assumed value of 0.1. However, image-to-image variations in THEMIS thermal inertia persist despite the use of measured opacities. This suggests that the offset in Figure 2 is not caused by incorrect opacity information and probably has some other source.

References: [1] Jakosky, B. M. *et al* (2003) *Eos Trans.* 84(46) Abs. P21C-03. [2] Mellon, M. T. *et al* (2000) *Icarus* 148. [3] Christensen, P. R. *et al* (in press) *Spac. Sci. Rev.* [4] Tillman, J. E. *et al* (1993) *JGR* 98 E6. [5] Putzig, N. E. *et al* (2003) *LPSC XXXIV* 1429. [6] Smith, M. D. *et al* (2001) *JGR* 106 E10. [7] Martínez-Alonso, S. *et al* (2004) *LPSC XXXV*. [8] Hynek, B. M. *et al* (2004) *LPSC XXXV*. [9] Murphy, N.W. *et al* (2004) *LPSC XXXV*.